Proceedings of the 7th International Symposium on Remote Sensing of Environment Ann Arbor 1971 May 17-21

SPECTRAL PARAMETERS AFFECTING AUTOMATED IMAGE INTERPRETATION USING BAYESIAN PROBABILITY TECHNIQUES

William G. Brooner

Department of Geography
University of California
Riverside, California 92502

Robert M. Haralick and Its'hak Dinstein

Department of Electrical Engineering
and Center for Research, Inc.
University of Kansas
Lawrence, Kansas 66044

ABSTRACT

This paper reports results on the implementation of a Bayesian Decision Rule to the identification of remotely sensed data. The Bayes programs were developed at the University of Kansas and are part of the KANDIDATS system (Kansas Digital Image Data System). A simple Bayesian Decision Rule is one which assigns a resolution cell having pattern measurements d to that category whose conditional probability, given measurement d, is highest.

The remotely sensed data used in this study consisted of very high altitude (approximately 65,000 feet) 35 mm Infrared Ektachrome and black and white multiband photography flown in the NASA/MSC Hi-Flight program in March 1969, over the Imperial Valley, California.

Several approaches to the identification of a variety of known agricultural land-use categories occurring in the study region were taken. First, multiple spot densitometric measurements were obtained from the color infrared photographs in each of the yellow, magenta, and cyan emulsion layers. These spot measurements integrated image densities over an area comparable to expected ERTS ground resolution cells. Identification was performed on the raw densitometric data as well as data standardized with respect to point intensity and linear transformations. The data sets were quantized to equally spaced levels or equally probable levels. The probability of correct identification was 60 to 70 percent for all data sets involved.

Second, identification of single emulsion black and white photographs were digitized to 64 grey levels by microdensitometric scanning at approximately 600 resolution cells per inch. Identification accuracy was 55 percent. When additional measurements were

included to account for within field micro-texture, identification improved to 65.6 percent, an increase of 14 percent.

Analysis of these data suggest the following conclusions: (1) approximately 70 percent correct identification accuracy can be achieved, (2) there is no general advantage to any of the particular quantizing and normalizing procedures tested, and (3) the spectral texture effects which occur at an extremely small image scale, can be used to increase the accuracy of land-use identification.

1. INTRODUCTION

Interpretation of small-scale remote sensor imagery, including high altitude and spacecraft photography, requires that certain techniques, which differ from larger scale imagery, be employed. Specifically, the elements of photo interpretation of small-scale imagery requires greater dependence upon photographic tone or color, shape and size, because resolution limitations often prevent the detection of texture or pattern even though they may exist. The interpretation and analysis of small-scale remote sensor imagery is complicated when one considers the quantities of data, both available and expected, from satellites and/or high altitude aircraft. The development of automated techniques alleviates some problems of retrieving, processing, and analyzing large volumes of remotely sensed data and therefore provides increasing flexibility to the reconnaissance of earth resources via remote sensors.

2. REMOTE SENSING PATTERN RECOGNITION PROBLEMS

Automated analysis of remotely sensed imagery is a special problem in pattern recognition. The human analogy to machine automation is the eye-brain system, which is the most efficient and complex pattern recognizer in existence. Although a number of decision rule techniques are available, the successful development of an automatic pattern recognizer is still in the future (Steiner, 1970) because the problem of automatically determining relevant pattern features for the decision rule is not yet solved. The present need is for studies to examine those environmental and image characteristics which provide relevant identification information with respect to the categories of interest.

Attempts to accurately identify discrete categories from remotely sensed imagery using pattern recognition techniques have been conducted by a number of researchers during the past few years. The successes at the Universities of Kansas, California (Berkeley), Michigan, and Purdue, for example, have been encouraging and have produced increased interest in various pattern recognition techniques using digitally transformed data from cameras, optical-mechanical and electronic scanners. (Brooner and Simonett, 1971; Fu et al., 1969; Haralick and Kelley, 1969; Lent, 1968; Rib and Miles, 1969; Steiner, 1969, 1970.)

Each of these attempts have used point value spectral or grey tone density as the relevant features and have not used those areal features of spectral or grey tone distribution which constitute texture. In this study we consider small areal spectral or tonal distribution parameters which measure micro-texture effects in addition to grey tone or color point density.

3. IMAGERY

Limited availability of small-scale photography restricts the selection of both study areas and categories for current research. Through the cooperation of the Forestry Remote Sensing Lab, University of California, Berkeley, imagery and

supporting ground data has been obtained from several high altitude missions of the NASA Earth Resources Survey Hi-Flight Program during 1969. Multiband imagery (Pan-25A, Pan 58, IR-89B, and Infrared Ektachrome) was obtained using a cluster of four 35 mm Nikon cameras (21 mm focal-length). Flight altitude for each mission was approximately 65,000 feet above terrain with a resulting photo scale for the 35 mm photographs of approximately 1/600,000. The mission used in this study was flown March 8, 1969, over the Imperial Valley, California. Representative photographs are shown in Figure 1.

Ground truth data was collected in a 12 square mile study area for the date of photographic coverage. These data consisted of the recorded crop-type, land-use, and notations of crop maturity for each of 160 field units. Although a large variety of crops are grown in this area during a calendar year, only eight crop-types or land uses were recorded for the March photography. Figure 2 shows the land-use in the study area.

4. STUDY AREA

The study area for the high-altitude sequential photography is a 12 square mile area in the Imperial Valley, California. Land-use throughout is intensive, irrigated agriculture. The Imperial Valley study area is significant to the present program for several reasons: First, and perhaps foremost, is the aforementioned availability of small-scale sequential photographic coverage. Second, the presence of several or more fields of the same land-use to allow investigation of within category variations in spectral reflection. Third, the presence of a variety of similar categories (i.e., multiple crops) to allow such applications as training and predicting of category identification. Fourth, the absence of natural rainfall allowing controlled soil and vegetation moisture within field units.

5. GROUND TRUTH

Several questions need to be briefly considered regarding "Ground Truth" data. First, is the time of data survey and collection relative to the photographic overflight. Second, is the type of crop condition data being gathered. Third, are the problems of within field variation in crop condition. And last, are the problems of variation due to soil conditions, i.e. moisture, salinity, and structure.

The time factor of flight date versus ground truth date can be very important. Of several dates given preliminary examination in this study, only in one case was the photography and ground truth obtained on the same day. An extreme was reached when the nearest date of ground truth gathering to flight date was one in which ground truth was gathered 12 days before the flight. The importance of these discrepancies to the study comes when these intervals coincide with rapid crop growth or harvesting of crops and thus effect spectral reflectance.

Related to this is the question of the type of ground truth being gathered. Rather than using terms varying from "very, very young to mature" which seems to appear vague and indeterminant from the perspective of high-altitude photos, other terms such as percent of field cover, plant height or coloration, and maturity condition might increase the accuracy of identification results. For example, there is virtually no difference between any crop in a very young condition in terms of percent ground cover, and furthermore, this condition is essentially bare soil.

In addition, the data must be schematized for the local region. In the Imperial Valley, for example, alfalfa and rye are often planted together, the rye seed holding the alfalfa until the latter commences growth. It is unnecessary to record fields as separate categories of alfalfa, rye, alfalfa-rye, or even grass. Rather, it is sufficient in this region to record all as alfalfa, thus eliminating redundancy, confusion, and small sample size problems. Similar situations occur in other agricultural regions and must be given these field survey considerations.

Within field variation of the crops is significant in a number of fields due, no doubt, to a variety of factors inherent in farming activities in the area. This creates a problem of both reading densitometric data and gathering ground truth, and in turn affects the accuracy of the results.

The last problem deals with soil conditions and is very noticeable in a large number of fields. This is probably due to poor soil structure and farming techniques. The results are ponding and deposition of salts which in turn influence plant growth and ultimately affect the accuracy of the information obtained.

It is virtually impossible to account for all minute variations which can and do occur in an agricultural region. Rather, the data collected must be used to best advantage, often by generalizing more meaningful data groups. To arrive at new data groups, decision rules must be used which consider the data gathering ability of the remote sensor device being employed.

Any regrouping of data and generation of new categories must meet two criteria. First, the new categories must be meaningful to both the sensor, the user of the data and classification scheme. Second, the new categories must restructure the data in such a manner as to significantly increase the accuracy of previous classifications. Shown in Table 1 is an example of data regrouping. Since all land-use data is referenced to a five digit code, data can be generalized to the fourth digit, and so on.

6. DENSITOMETRY

Spot densitometric measurements were made on selected Infrared Ektachrome photographs by sampling in each of the 160 fields present in the area. Variations of spectral reflection for each category were then determined and compared.

Filters used in the density measurements were Wratten 47B, 92, and 99. This enabled very crude - but acceptable for the purposes of this study - "simulation" of multiband photography employing discrete bands in the green, red, and near infrared regions.

A Macbeth Quantalog Photographic Color Analyzer with a 1 mm transmission aperture was used to measure color density. Because the individual fields on the 35 mm transparencies of 1:600,000 scale were too small to be measured with a 1 mm transmission aperture, color transparency enlargements of the study area were made to a scale of approximately 1:94,000. This was a reluctant, yet necessary, procedure because further generations of photography (particularly enlargement) may cause image degradation and may increase within category variations. The area illuminated through a 1 mm aperture corresponds to a small-area ground patch of approximately 300 ft. diameter.

Samples were taken according to field size in the following manner: fields less than 40 acres = 3 samples; 40 acres = 5 samples; 80 acres = 8 samples; 160 acres = 16 samples. Table 2 shows the number of samples obtained for each data of photography; for each sample three measurements were obtained representing the yellow, magenta, and cyan values. These measurements constitute one set of raw data.

Another set of densitometric measurements were made on three multiband black and white images covering the same spectral bands as the IR Ektachrome image. However, these densitometric measurements were made by a scanning densitometer designed and built at the University of Kansas. The scanning densitometer has a spot size of about 70 microns and samples a grey tone about every 50 microns. It digitized each grey tone to sixty-four levels and recorded the digitization on magnetic tape. Before digitization took place amplifier gain and offset was adjusted so that the darkest and lightest grey tones were digitized to the smallest and largest binary numbers within the sixty-four levels set. This, in essence,

provided an equal interval quantization.

7. DATA NORMALIZATION

One serious problem in many remote sensor-environment systems is the lack of consistent calibration from sensor to sensor and from day to day. Photographic sensors are particulary plagued with calibration problems since no controlled attempt is usually made to compensate for exposure, lens, film, developer, print and off-axis illumination fall off differences. The environment compounds the problem by varying atmospheric variables such as haze and cloud cover.

Pettinger (1969) documented this variability in image quality which occurred from the mission used in this study and from several other missions on several dates for multispectral photography in the Phoenix area. He ascribed color balance variability to exposure, film (age and storage), and processing differences.

There are several ways to operate on such uncalibrated imagery to bring it into various normalized forms. One way is to do equal interval quantizing.

To perform equal interval quantizing the lighest grey tone, l, and darkest grey tone, d, on the image are determined. The range $d-l$ of grey tones is then divided into K equal intervals, each of length $(d-l/K)$. Any grey tone lying between l and $l + (d-l/K)$ is assigned to the first quantized level Q_1. Any grey tone lying between $l + (d-l/K)$ and $l + 2(d-l/K)$ is assigned to the second quantized level Q_2. In general, any grey tone lying between $l + (m-1)(d-l/K)$ and $l + m(d-l/K)$ is assigned to the m^{th} quantized level Q_m.

Images whose grey tones have been discretely quantized in this manner are invariant with respect to linear grey tone transformation. To explain what this means, let us assume for example that we have a black and white image which we consider calibrated. Let us also assume that we have a second image, just like the first, except that it is uncalibrated. (Perhaps it had been in the developer too long or it is visibly pre-fogged etc.) If we can assume that the gamma change can be described by a simple scaling effect and that the overall darker (or lighter) appearance can be described by the addition or subtraction of some grey tone, then the quantized pictures obtained by equal interval quantizing will be the same for the calibrated and uncalibrated image.

It is easy to understand why equal interval quantizing is invariant with respect to linear transformations. Let $\{X_1, X_2, \ldots, X_n \mid X_i \leq X_{i+1}\}$ be the ordered set of grey tones for the calibrated image and $\{Y_1, Y_2, \ldots, Y_m \mid Y_i \leq Y_{i+1}\}$ be the ordered set of grey tones for the uncalibrated image. For equal interval quantizing, the m^{th} quantized level Q_m of the calibrated image is defined as the set

$$Q_m = \left\{ X \mid X_1 + (m-1)\frac{(X_n - X_1)}{K} \leq X < X_1 + m\frac{(X_n - X_1)}{K} \right\}$$

and the m^{th} quantized level Q'_m of the uncalibrated image is defined as the set

$$Q'_m = \left\{ Y \mid Y_1 + (m-1)\frac{(Y_n - Y_1)}{K} \leq Y \leq Y_1 + m\frac{(Y_n - Y_1)}{K} \right\}.$$

Because we assume the uncalibrated image is a linear transformation of the calibrated image we must have, $y = ax+b$, where $a > 0$. ($a < 0$ would imply the uncalibrated image is a negative). Now, $Y \in Q'_m$ if and only if

$$ax_1 + b + \frac{(m-1)(ax_n + b - ax_1 - b)}{K} \leq ax + b < ax_1 + b + \frac{m(ax_n + b - ax_1 - b)}{K}.$$

First subtracting b from these inequalities and then dividing by a, we obtain

$$Y \in Q'_m \quad \text{if and only if} \quad X_1 + (m-1)\frac{(X_n - X_1)}{K} \leq X < X_1 + \frac{m(X_n - X_1)}{K} ,$$

and this happens if and only if $X \in Q_m$. This says that if we collect all the grey tones which were put into the m^{th} quantized interval on the calibrated image and then transform each of these grey tones to what they would be on the uncalibrated image, then we would find that these would be the grey tones in the m^{th} quantized interval on the uncalibrated image. Hence, the quantized calibrated and uncalibrated pictures would be the same.

For color images, each emulsion may be quantized as a black and white image would be quantized to achieve a color balance normalization. However, this is not the only type of normalization applicable to color images. Sometimes, due to camera design, illumination across the film is not uniform. More light energy falls on the center of the film than on the edges (off-axis illumination fall-off). If the assumption can be made that the relevant information is in hue and not in color intensity, then for any place on the color film, the densities of each of the three emulsions can be divided by the sum of the emulsion densities at that location. Since the sum of the densities is proportional to color intensity, this intensity normalization standardizes each place on the film to the same intensity. As with the equal interval quantization procedure, if we compared a normalized calibrated image to a normalized uncalibrated image (one with off-axis illumination fall-off) we would find that intensity normalization would make the two identical.

8. THE BAYES DECISION RULE

One approach to the discrimination problem involves the use of a simple Bayes Decision Rule. Such a rule assigns the data point d to the most "likely" land-use category. That is, if d is a three-dimensional vector, of data taken from IR Ektachrome film, whose first component is the spectral reflectance from the cyan emulsion (700-900 nm), whose second component is the spectral reflectance from the magenta emulsion (590-690 nm), whose third component is the spectral reflectance from the yellow emulsion (490-590 nm), and if c is any land-use category, then the Bayes Decision Rule assigns the measurement d to the category c^* if and only if the conditional probability of c^* given d is greater than or equal to the conditional probability of c given d for any category c. If we denote the conditional probability of category c given measurement by $P_d(c)$, then the above condition may be written as

$$P_d(c^*) \geq P_d(c) \quad \text{for every category } c .$$

Now, by Bayes formula,

$$P_d(c) = \frac{P_c(d)P(c)}{P(d)}$$

where $P_c(d)$ is the conditional probability of d given c and $P(c)$ is the probability of c. Hence, d is assigned to category c^* if

$$\frac{P_{c^*}(d)P(c^*)}{P(d)} \geq \frac{P_c(d)P(c)}{P(d)}$$

for every land use category c. Since $P(d) \geq 0$, we may multiply both sides of the inequality by $P(d)$ and obtain that the Bayes rule assigns d to category c^* if

$P_{c^*}(d)\,P(c^*) \geq P_c(d)\,P(c)$, for every land-use category c.

The probability $P(c)$, called the prior probability, is the probability that the land-use category c occurs.

When the images are quantized, to say K levels, then each component of d can take on K possible values. If there are N components to each measurement, then the number of possible measurements is N^K. If there are M land-use categories, then $M \cdot N^K$ is the number of memory locations necessary to store the set of conditional probabilities $P_c(d)$. This number exponentially increases with K and is often so large that it is either uneconomical or inconvenient to provide quick access to that number of computer memory locations when making estimates of $P_c(d)$. In this case it is convenient to assume that $P_c(d)$ takes some particular functional form of a continuous distribution where the distribution can be specified by a few parameters. The usual distributional form is the multivariate normal distribution (Fu, et al., 1969) that is,

$$P_c(d) = \frac{1}{(2\pi)^{u/2}|\Sigma_c|^{\frac{1}{2}}} e^{-\frac{1}{2}(d-\mu_c)'\Sigma_c^{-1}(d-\mu_c)}$$

where $\Sigma_c = E[(d-\mu_c)(d-\mu_c)']$ is the covariance matrix for measurements coming from category c and $\mu_c = E[d]$ is the mean value of the measurements coming from category c.

The covariance matrix is estimated by

$$\hat{\Sigma}_c = \frac{1}{J}\sum_{n=1}^{J}(d_n-\hat{\mu}_c)(d_n-\hat{\mu}_c)'$$

and the mean is estimated by

$$\hat{\mu}_c = \frac{1}{J}\sum_{n=1}^{J} d_n .$$

where $d_1, d_2, \ldots d_j$ are all measurements coming from land-use category c and x' denotes the transpose of the vector x.

The advantage of using the Bayes rule in the discrete form is that no assumptions need be made about the form of the conditional probability distributions. Thus, it is a very general technique. The advantage to using the Bayes rule in the continuous form is that only a small amount of memory storage is needed to store the conditional probabilities. Thus, it is an efficient technique. The disadvantage of the discrete form is the large number of memory locations needed to store the conditional probabilities in addition to the fact that often there are not enough samples available to get good estimates for the conditional probabilities. The disadvantage of the continuous form is the restricted condition under which it may be used -- the data must fit the distributional form for the results to be valid.

In this paper we will make some comparisons between the continuous and discrete forms.

9. ANALYSIS AND RESULTS

The raw spot densitometric data consisting of 883 points for each of the three emulsions of the Infrared Ektachrome film, and the intensity normalized spot densitometric data were quantized two ways: by ten level equal interval and ten level equal probability quantizing. The data were then processed by the discrete Bayes rule where the prior category probabilities were set to their actual frequency of occurrence in the study area. The data set was divided in half. The first half (called the training set) was used to estimate the conditional probabilities and the second half (called the prediction set) was identified using the discrete Bayes rule determined by the first half.

The classification results for the Infrared Ektachrome film and spot densitometric data using a discrete Bayesian approach are shown in Tables 3 through 6. Table 3 presents contingency tables showing the full classification matrix for the prediction set of each data set. Summary results are shown in Table 4 for the training and prediction set of various data sets.

The results in each example are generally similar. In the training sets the identification accuracy was consistently in the middle 70 percent, with the normalized data generally slightly higher percentage than the raw data (74 percent compared to 76 percent). The prediction set results were 5 to 10 percent lower, ranging from 61 percent to 71 percent correct identification.

Also shown on the contingency tables are the Type I (omission) and Type II (commission) errors for each category. The probability of Type I errors in class i is defined as the number of data elements belonging but not assigned to category i divided by the total number of elements belonging to category i. The probability of Type II errors in category i is defined as the number of elements assigned but not belonging to category i, divided by the total number of elements assigned to category i.

The performance of various processing techniques on different categories (crops) may be compared by examining the Type I and Type II errors, Tables 5A and 5B. There are several differences, as exemplified by the Alfalfa category. The equally spaced quantizing and normalization procedure yielded the lowest percentage of Type I errors (14 percent), but also the highest percentage of Type II errors (35 percent) for the Alfalfa category. Type I errors may often be traded for Type II errors and vice versa. Similar comparisons may be made for other categories.

The above data illustrate the results for the identification of crops throughout the study area. Essentially, this is a frequency accuracy which, as Steiner (1969) has stated, is "a statistical summary for the study area only and not in the actual location of (land use categories)...". Location accuracy is a necessary prerequisite for the implementation of sequential remote sensor and environmental data in some sort of a "Geographical Information System." Since each data point is examined and classified individually in this analysis it is also possible to consider location accuracy. Figure 3 shows those fields in the study area which were correctly and incorrectly identified in the Equally Spaced Quantized raw data prediction set. Rather than illustrate the identification for each field, only four categories are shown: correct identification; two categories of incorrect identification consisting of completely wrong, and undecided, where there was an equal decision between correct and incorrect identification of data points within the field; and a few fields which were not examined and identified. The individual crop-types in the correct fields may be found by referring to the Ground Truth Map (Figure 2). Of the 160 fields in the study area, 108 were correctly identified, yielding a location accuracy in this example of 68 percent.

Discussed above was the application of data regrouping and the example given was to regroup to a high order of land-use, or in this case extensive versus intensive agriculture, based on a five digit code. To illustrate the effects and uses of

this data regrouping, consider the results of the Equally Spaced Quantized raw data shown in Table 3A. These eight categories are of the fifth digit order. Regrouping to the fourth digit order yields the same results since no categories are combined. Regrouping to the third digit order, however, reduces the eight crop-type categories to four crop-group categories and yields a higher percent correct identification. While previously there were 307 of 441 or 70 percent of the data points correctly identified, now there are 392, or 88 percent, correctly identified data points, as shown on Table 6. Similarly, in the Equal Probability Quantized raw data, there were 61 percent correctly identified crop-type data points. Regrouping to the third order digit yields a correct identification of 86 percent. Regrouping by combining categories will always yield correct percentage results which are equal to or greater than the uncombined categories. Justification, however, must consider the advantages and benefits, if any, of such aggregate data.

The raw scanning densitometric data of the multiband photography were processed by two methods. In each method the data set was divided randomly in half, the first half being used for training and the second half being used for prediction. One method used approximately 20,000 grey densities obtained on a resolution cell by resolution cell basis to make land-use decisions on a resolution cell by resolution cell basis. This method treats each resolution cell independently, ignoring the local dependence of nearby resolution cells. The discrete form of the Bayes rule yielded 55 percent correct identification on the prediction set, and the continuous form of the Bayes rule also yielded 55 percent. Figure 4 depicts the decision rule boundaries used by the discrete Bayes rule.

The other method was to make decisions on a small area basis taking into account that micro-texture is produced by tonal variations as well as by the average tone. The training set was divided into small area patches of 25 randomly chosen resolution cells and the first, second, and third moments of these samples were estimated. The nine measurement components then consisted of the first three moments for each small-area patch for each multiband photograph. The continuous form of the Bayes rule yielded 66 percent correct identification on the prediction set. To test if the mean averaging (first moment) caused the accuracy increase and whether the additional discrimination had been provided by the second and third moments, we reprocessed the data set using only first moment and using only first and second moments. The continuous form Bayes rule yielded 58 percent correct identification on the prediction set using only the first moment and 65 percent correct identification on the prediction set using only the first and second moments. Hence, the second moment (variance) provided the most significant increase in identification accuracy.

Image texture is concerned with the frequency and range of tone change and/or with the spatial geometric arrangement of tones. The micro-texture effect found in this photography is not due to any spatial geometric arrangement of tones, nor is it due to the frequency of tone change. Rather, the texture effect is one of a range of tones. The heterogeneity of both alfalfa and bare soil, for example, reflected itself in a wider range of grey tones around its respective means than of the other more homogeneous land-use categories in this data. Hence, the grey tone variance (second central moment) in any small-area patch was relatively higher for alfalfa and bare soil than for the other land-use categories. This higher variance provided additional information for a 15 percent increase in identification accuracy.

The classification results for the multiband photography densitometric data are shown in Tables 7 through 9. As in the previous discussion of the Infrared Ektachrome film, contingency tables are shown in Table 7. These display the full classification matrix for the prediction set of the various data sets and analysis techniques. Summary results are shown in Table 8 for the training and prediction sets for each technique.

The range of results is much larger than in the previous discussion. The training set data varies from 49 percent to 82 percent correct identification of land-use categories, and the prediction set data has a similar range from 43 percent to 66 percent correct identification.

Tables 9a and 9b summarize the Type I and Type II errors for these prediction set data. The percentage of error for each category was generally the same for both Type I and Type II. The only land-use category identified with minimal omission (Type I) errors was bare soil, which occurred when using both the first moment, and the first and second moments, and all three moments in the analysis. The highest occurrence of omission (Type I) errors generally occurred when only a single parameter was employed. This also resulted in large commission (Type II) errors.

When all three moments were used in the classification analysis, the result was 66 percent correct identification. When only the first and second moments were employed in the classification analysis, 65 percent correct identification resulted. The best results occurred when the first moment was used with the second moment or the second and third moments. Any combination without the first moment generally resulted in relatively inferior results.

A comparison of results from the Infrared Ektachrome film and the multiband films suggest that the Infrared Ektachrome film yielded slightly higher results. The difference, however, between the best results from the Infrared Ektachrome film (normalized data, Equal Probability Quantizing = 71 percent correct identification), and the best result from the multiband film (all three moments = 66 percent correct identification) is a difference of only 4 percent.

Several other studies have recently been conducted with these and similar data in the Imperial Valley, and with similar data in the Phoenix, Arizona region. The high altitude overflight acquiring imagery used in this study concurred and supported the Apollo IX SO-65 experiment. In a recent study by Wiegand et al. (1971) at the Agricultural Research Station, Weslaco, Texas, Apollo IX photographs of the Imperial Valley were examined. Densitometric data from isodensity traces on the photographs were used to classify rural land use and yielded results similar to those presented above. Overall correct identification was 68 percent for Infrared Ektachrome film and 72 percent for the multiband films. Wiegand discriminated among five categories, four of which are the same as the present study (sugar beets, alfalfa, bare soil, and barley; the fifth was salt flat). Among Wiegand's conclusions were: (a) crop heights vary considerably but do not seem related to proper crop identification; and (b) larger fields seem easier to identify than smaller fields.

Steiner has recently been working with the same spot densitometric data of the Infrared Ektachrome film of this study. A variety of discriminant analysis experiments have been performed for land use identification, all yielding generally inferior results. A Cosine-Theta classification, whereby group centroids are calculated and classification of test data is based on angular proximity to centroids, yielded a 41 percent correct identification. A Linear Discriminant Analysis, using the assumption of normal distributions and equal covariances, yielded a 37 percent correct identification. A Nearest Neighbor Classification, whereby classification of test data is based on minimum distance to individual sample points, also yielded a 37 percent correct identification. Steiner's results suggest that the spot densitometric data consists of categories whose boundaries were non-linear. Examination of the optimal decision boundaries in Figure 4 show categories such as alfalfa and barley not separable by linear boundaries and this indeed was one area where Steiner's linear discriminant function failed to achieve good identification. Using the same data in a continuous Bayes program with quadratic boundaries yielded 45 percent identification.

Finally, recent efforts at the University of California, Berkeley, and reported by Lauer (1971), have been directed toward the use of photo-interpreters to discriminate land-use categories from high altitude photography of the same mission used in this study. The test site, Phoenix, Arizona was different, but contains several common characteristics as an arid agricultural region. These studies have found that the use of multiband photographs on single dates produce generally low overall photo-interpretation results. In March for example the red sensitive emulsion (Pan 25A) yielded 48 percent and the near-infrared sensitive emulsion (IR 89B) yielded 45 percent correct identification. Overall interpretat results improved when single date photographs were viewed in multi-emulsion form (i.e. Infrared Ektachrome or optical color combination) and when multiband photographs taken on two dates were optically color combined. The March Infrared Ektachrome photograph yielded a 64 percent correct photo-interpreter identificati

10. CONCLUSIONS

The data analysis discussed above has considered a Bayesian Decision Rule to the automated identification of remotely sensed data. These data consisted of densitometric measurements of Infrared Ektachrome and multiband small scale aeria photographs. It has been demonstrated that approximately 70 percent accuracy can be achieved when identifying certain land-use categories from Infrared Ektachrome films. When using multiband films, results of 66 percent accuracy have been achieved. The use of various quantizing and normalization procedures yielded generally similar results. Their differences do not seem to justify the exclusi use of any particular procedure. Finally, when collecting point density data fr small scale imagery, minute spectral texture information exists. The informatio when added to tonal (or density) data can be used to increase the accuracy of land-use identification.

11. ACKNOWLEDGEMENTS

This study has been carried out under the support of the following organizations: (1) At the University of California, Riverside: Project THEMIS, Department of the Navy, Office of Naval Research, Geography Programs Branch. Contract No. N00014-69-A-0200-5001. (2) At the University of Kansas: Project THEMIS, Department of the Army, U. S. Army Topographic Command, Corps of Engineers Engineering Topographic Laboratories, Fort Belvoir, Virginia. Contract No. DAAK02-68-C-0089. Computations were carried out at the University of California, Riverside, Computer Center, and at the Kansas University Computer Center. NASA imagery and ground truth data was provided by the Forestry Remote Sensing Laboratory, School of Forestry and Conservation, University of California, Berk

12. REFERENCES

Brooner, W. G. and D. S. Simonett (1971). "Crop Discrimination with Color Infrared Photography," Journal of Remote Sensing of the Environment. In Press.

Fu, K. A., D. A. Langrebe, and T. L. Phillips (1969). "Information Processing of Remotely Sensed Agricultural Data," Proceedings of the IEEE, LVII, 4 (April), pp. 639-653.

Haralick, R. M. and G. L. Kelley (1969). "Pattern Recognition with Measurement Space and Spatial Clustering for Multiple Images," Proceedings of the IEEE, LVII, 4 (April), pp. 654-665.

Lauer, D. T. (1971). "Testing Multiband and Multidate Photography for Crop Identification." Presented at the International Workshop on Earth Resources Survey Systems, Ann Arbor, Michigan, May 3-14, 1971.

Lent, J. D. (1968). The Feasibility of Identifying Wildland Resources Through the Analysis of Digitally Recorded Remote Sensing Data. Annual Progress Report. Forestry Remote Sensing Laboratory, School of Forestry and Conservation, University of California, Berkeley.

Pettinger, L. R. et al. (1969). Analysis of Earth Resources on Sequential High Altitude Multiband Photography. A special report prepared for the Office of Space Sciences and Applications, NASA, by personnel of the School of Forestry and Conservation, University of California, Berkeley.

Rib, H. T. and R. D. Miles (1969). "Automatic Interpretation of Terrain Features," Photogrammetric Engineering, XXXV, 2 (February), pp. 153-164.

Steiner, D. (1969). "Computer-Processing and Classification of Multi-Variate Information from Remote Sensing Imagery," Proceedings of the Sixth International Symposium on Remote Sensing of Environment. October, 1969, Ann Arbor, Michigan. pp. 895-907.

Steiner, D. (1970). "Automation in Photo Interpretation," GEOFORUM, 2, pp. 75-88.

Wiegand, C. L., R. W. Leamer, D. A. Weber, and A. H. Gerbermann (1971). "Multibase and Multiemulsion Space Photos for Crops and Soils," Photogrammetric Engineering, XXXVII, 2 (February), pp. 147-156.

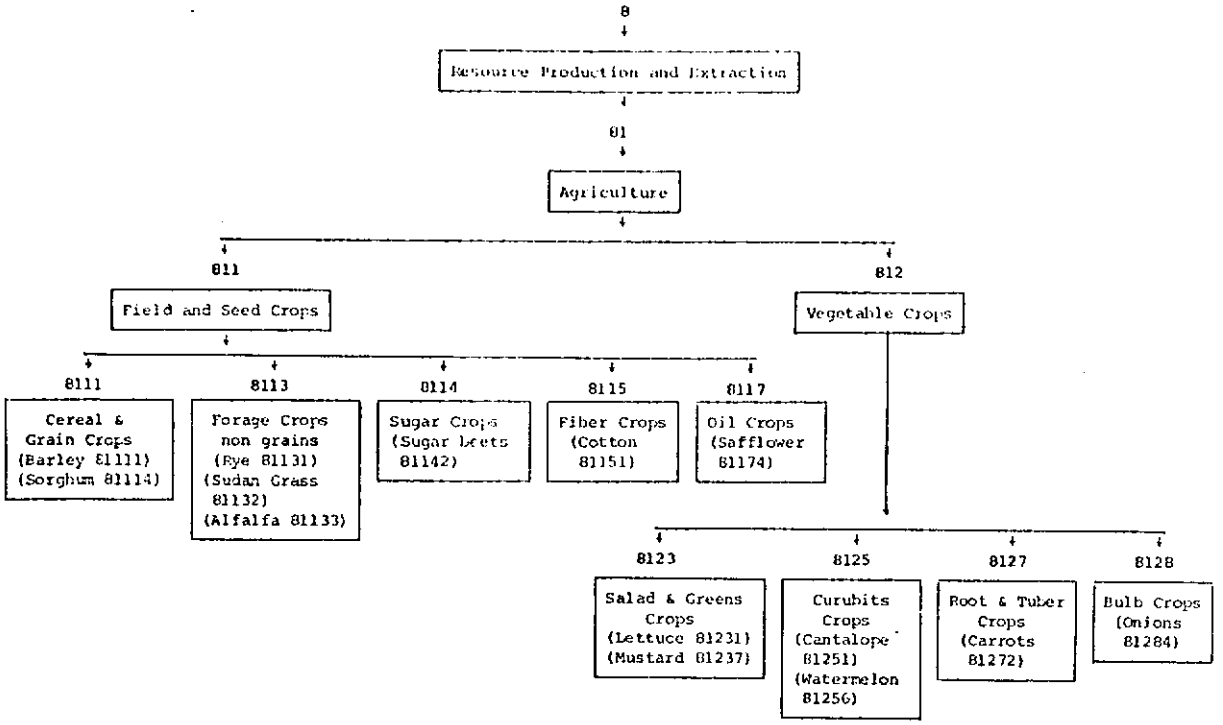

TABLE 1. An example of land-use data regrouping based on a five digit hierarchical classification. Source: Standard Land Use Coding Manual, Urban Renewal Administration.

CATEGORY	# UNITS	%	# DATA POINTS	%
Alfalfa*	65	40.6	365	41.3
Barley	33	20.6	181	20.5
Safflower	5	3.1	20	2.3
Sugar beets	9	5.6	57	6.4
Lettuce	7	4.4	36	4.1
Onions	3	1.9	15	1.7
Pasture	5	3.1	20	2.3
Bare soil	33	20.6	189	21.4
Total	160		883	

*Includes both cut and mature alfalfa, as well as alfalfa seeded with rye grass.

TABLE 2. Distribution of crop-types and spot densitometric data points in each emulsion layer of the Infrared Ektachrome image used in this study.

3A

TRUE CLASS \ CLASSIFIED AS	A	B	SF	SB	L	O	P	BS	OMISSION TOTAL	OMISSION ERROR	OMISSION %
A	153	21	4				1	4	183	30	16
B	31	56						1	88	32	36
SF	5		3					2	10	7	70
SB	16	8		4					28	24	86
L	10	1						8	19	19	100
O		1						7	8	8	100
P	9						1		10	9	90
BS	5							90	95	5	5
COMMISSION TOTAL	230	87	7	4			2	122	441		
COMMISSION ERROR	77	31	4				1	22		134	
COMMISSION %	33	36	57				50	20			70

3B

TRUE CLASS \ CLASSIFIED AS	A	B	SF	SB	L	O	P	BS	OMISSION TOTAL	OMISSION ERROR	OMISSION %
A	157	9	5	1	8			3	183	26	14
B	37	49			2				88	39	44
SF	7	1						2	10	10	100
SB	20	7	1						28	28	100
L	9				8			2	19	11	58
O	1				2			5	8	8	100
P	10								10	10	100
BS					1			94	95	1	1
COMMISSION TOTAL	241	66	6	1	21			106	441		
COMMISSION ERROR	84	17	6	1	13			12		133	
COMMISSION %	35	26	100	100	62			11			70

3C

TRUE CLASS \ CLASSIFIED AS	A	B	SF	SB	L	O	P	BS	OMISSION TOTAL	OMISSION ERROR	OMISSION %
A	112	36	13	6	1		3	12	183	71	39
B	26	56		3	2			1	88	32	36
SF	2	1	5					2	10	5	50
SB	12	13		3					28	25	89
L	5	1	1		2		1	9	19	17	89
O	1	1						6	8	8	100
P	6	1	3						10	10	100
BS						5		90	95	5	5
COMMISSION TOTAL	164	120	22	12	5	5	4	120	441		
COMMISSION ERROR	52	30	17	9	3	5	4	30		173	
COMMISSION %	31	25	77	75	60	100	100	25			61

3D

TRUE CLASS \ CLASSIFIED AS	A	B	SF	SB	L	O	P	BS	OMISSION TOTAL	OMISSION ERROR	OMISSION %
A	143	15	1	6	3	1	10	4	183	40	22
B	23	56		7	1			1	88	32	36
SF	3		3	1			1	2	10	7	70
SB	8	13		6			1		28	22	79
L	11				6			2	19	13	68
O					1		1	6	8	8	100
P	7		1				2		10	8	80
BS					1			94	95	1	1
COMMISSION TOTAL	196	84	5	20	12	1	15	109	441		
COMMISSION ERROR	52	28	2	14	6	1	12	15		130	
COMMISSION %	27	33	40	70	50	100	87	14			71

TABLE 3. Classification results for the Infrared Ektachrome spot densitometric data. The contingency tables show the full classification matrix for the prediction sets of: (A) raw data, equal space quantized; (B) normalized data, equal space quantized; (C) raw data, equal probability quantized; and (D) normalized data, equal probability quantized.

DATA	TRAINING SET			PREDICTION SET		
	#TOTAL	#CORRECT	%	#TOTAL	#CORRECT	%
Raw, E.S.Q.	442	392	74	441	307	70
Normalized, E.S.Q.	442	337	76	441	308	70
Raw, E.P.Q.	442	329	74	441	268	61
Normalized, E.P.Q.	442	334	76	441	311	71

TABLE 4. Summary of training and prediction results for the Infrared Ektachrome spot densitometric data sets.

TYPE I ERRORS (omission)

DATA	ALFALFA			BARLEY			SAFFLOWER			SUGAR BEET			LETTUCE			ONION			PASTURE			BARE SOIL		
	TOTAL	ERRORS	PER CENT	TOTAL	ERRORS	PER CENT	TOTAL	ERRORS	PER CENT	TOTAL	ERRORS	PER CENT	TOTAL	ERRORS	PER CENT	TOTAL	ERRORS	PER CENT	TOTAL	ERRORS	PER CENT	TOTAL	ERRORS	PER CENT
Raw, E.S.Q.	183	30	16	88	32	36	10	7	70	28	24	86	19	19	100	8	8	100	10	9	90	95	5	5
Normalized, E.S.Q.	183	26	14	88	39	44	10	10	100	28	28	100	19	11	58	8	8	100	10	10	100	95	1	1
Raw, E.P.Q.	183	71	39	88	32	36	10	5	50	28	25	89	19	17	89	8	8	100	10	10	100	95	5	5
Normalized, E.P.Q.	183	40	22	88	32	36	10	7	70	28	22	79	19	13	68	8	8	100	10	8	80	95	1	1

TYPE II ERRORS (commission)

DATA	ALFALFA			BARLEY			SAFFLOWER			SUGAR BEET			LETTUCE			ONION			PASTURE			BARE SOIL		
	TOTAL	ERRORS	PER CENT	TOTAL	ERRORS	PER CENT	TOTAL	ERRORS	PER CENT	TOTAL	ERRORS	PER CENT	TOTAL	ERRORS	PER CENT	TOTAL	ERRORS	PER CENT	TOTAL	ERRORS	PER CENT	TOTAL	ERRORS	PER CENT
Raw, E.S.Q.	230	77	33	87	31	36	7	4	57	4									2	1	50	112	22	20
Normalized, E.S.Q.	241	84	35	66	17	26	6	6	100	1	1	100	21	13	62							106	12	11
Raw, E.P.Q.	164	52	31	109	53	49	22	17	77	12	9	75	5	3	60	5	5	100	4	4	100	120	30	25
Normalized, E.P.Q.	196	52	27	84	28	33	5	2	40	20	14	70	12	6	50	1	1	100	15	12	87	109	15	14

TABLE 5. Summary of (A) Type I (omission) and (B) Type II (commission) errors for the Infrared Ektachrome spot densitometric data sets.

6A

TRUE CLASS	CLASSIFIED AS: F&S	V	P	BS	OMISSION TOTAL	OMISSION ERROR	OMISSION %
F & S	301		1	7	309	8	3
V	12			15	27	27	100
P	9		1		10	9	90
BS	5			90	95	5	5
COMMISSION TOTAL	327		2	112	441		
COMMISSION ERROR	26		1	22		49	
COMMISSION %	8		50	20			88

6B

TRUE CLASS	CLASSIFIED AS: F&S	V	P	BS	OMISSION TOTAL	OMISSION ERROR	OMISSION %
F & S	288	3	3	15	309	21	6
V	9	2	1	15	27	25	93
P	10				10	10	100
BS		5		90	95	5	5
COMMISSION TOTAL	307	10	4	120	441		
COMMISSION ERROR	19	8		30		61	
COMMISSION %	6	80		25			86

TABLE 6. Results are increased when data is regrouped to a higher order of land-use, as shown for the following Infrared Ektachrome spot densitometric data: (A) raw data, equal space quantized, and (B) raw data, equal probability quantized.

7A

TRUE CLASS \ CLASSIFIED AS	A	B	SF	SB	L	O	P	BS	TOTAL	ERROR	%
A	67	16		3	5	3	23		117	50	43
B	15	34	1	1	3		10		64	30	47
SF	2		1					2	5	4	80
SB	17	7	1	3					28	25	90
L					5	1	5	5	16	11	69
O					1	2		6	9	7	78
P	15	1	2				17		35	18	51
BS					2			70	72	2	3
TOTAL	116	58	5	7	16	6	55	83	346		
ERROR	49	24	4	4	9	4	38	13		147	
%	42	41	80	58	56	66	69	21			58

OMISSION

COMMISSION

7B

TRUE CLASS \ CLASSIFIED AS	A	B	SF	SB	L	O	P	BS	TOTAL	ERROR	%
A	57	10	3	1	3		38	5	117	60	51
B	22	17		6				19	64	47	73
SF	3		1				1		5	4	80
SB	9	10		7	1		1		28	21	75
L	2		1		1		4	8	16	15	94
O	4						2	3	9	9	100
P	7	7	4				16	1	35	19	54
BS	14			2	2	2	2	50	72	22	30
TOTAL	118	44	9	16	7	2	83	67	346		
ERROR	61	27	8	9	6	2	67	17		197	
%	52	61	89	56	86	100	81	25			43

OMISSION

COMMISSION

7C

TRUE CLASS \ CLASSIFIED AS	A	B	SF	SB	L	O	P	BS	TOTAL	ERROR	%
A	77	15		1	3		17	4	117	40	34
B	11	37		5			11		64	27	42
SF	2						1	2	5	5	100
SB	4	17		6			1		28	22	78
L					6		8	2	16	10	62
O	2						2	5	9	9	100
P	6	2					27		35	8	23
BS	1							71	72	1	1
TOTAL	103	71		12	9		67	84	346		
ERROR	26	34		6	3		40	13		122	
%	25	48		50	33		60	15			65

OMISSION

COMMISSION

7D

TRUE CLASS \ CLASSIFIED AS	A	B	SF	SB	L	O	P	BS	TOTAL	ERROR	%
A	80	16					18	3	117	37	32
B	15	38		3			8		64	26	41
SF							3	2	5	5	100
SB	8	9		11					28	17	61
L	4				1		7	4	16	12	75
O	3						1	5	9	9	100
P	3	3			1		27	1	35	8	23
BS	2							70	72	2	3
TOTAL	115	66		14	2		64	85	346		
ERROR	35	28		3	1		37	15		119	
%	30	42		21	50		58	18			66

OMISSION

COMMISSION

TABLE 7. Classification results for the multiband densitometric data. The contingency tables show the full classification matrix for the prediction sets of: (A) data of the first moment; (B) data of the second moment; (C) data of the first and second moments; and (D) data of the first, second, and third moments.

DATA	TRAINING SET			PREDICTION SET		
	#TOTAL	#CORRECT	%	#TOTAL	#CORRECT	%
1st Moment	346	235	68	346	199	58
2nd Moment	346	171	49	346	149	43
1st & 2nd Moments	346	270	78	346	224	65
1st, 2nd & 3rd Moments	346	285	82	346	227	66

TABLE 8. Summary of training and prediction results for the multiband densitometric data sets.

TYPE I ERRORS (omission)

DATA	ALFALFA			BARLEY			SAFFLOWER			SUGAR BEET			LETTUCE			ONION			PASTURE			BARE SOIL		
	TOTAL	ERRORS	PER CENT	TOTAL	ERRORS	PER CENT	TOTAL	ERRORS	PER CENT	TOTAL	ERRORS	PER CENT	TOTAL	ERRORS	PER CENT	TOTAL	ERRORS	PER CENT	TOTAL	ERRORS	PER CENT	TOTAL	ERRORS	PER CENT
1st Moment	117	50	43	64	30	47	5	4	80	28	25	90	16	11	69	9	7	78	35	18	51	72	2	3
2nd Moment	117	60	51	64	47	73	5	4	80	28	21	75	16	15	94	9	9	100	35	19	54	72	22	30
1st & 2nd Moments	117	40	34	64	27	42	5	5	100	28	22	78	16	10	62	9	9	100	35	8	23	72	1	1
1st, 2nd, & 3rd Moments	117	37	32	64	26	41	5	5	100	28	17	61	16	12	75	9	9	100	35	8	23	72	2	3

TYPE II ERRORS (commission)

DATA	ALFALFA			BARLEY			SAFFLOWER			SUGAR BEET			LETTUCE			ONION			PASTURE			BARE SOIL		
	TOTAL	ERRORS	PER CENT	TOTAL	ERRORS	PER CENT	TOTAL	ERRORS	PER CENT	TOTAL	ERRORS	PER CENT	TOTAL	ERRORS	PER CENT	TOTAL	ERRORS	PER CENT	TOTAL	ERRORS	PER CENT	TOTAL	ERRORS	PER CENT
1st Moment	116	49	42	58	24	41	5	4	80	7	4	58	16	9	56	6	4	66	55	38	69	83	13	21
2nd Moment	118	61	52	44	27	61	9	8	89	16	9	56	7	6	86	2	2	100	83	67	81	67	17	25
1st & 2nd Moments	103	26	25	71	34	48				12	6	50	9	3	33				67	40	60	84	13	15
1st 2nd & 3rd Moments	115	35	30	66	28	42				14	3	21	2	1	50				64	37	58	85	15	18

TABLE 9. Summary of (A) Type I (omission) and (B) Type II (commission) errors for the multiband densitometric data sets.

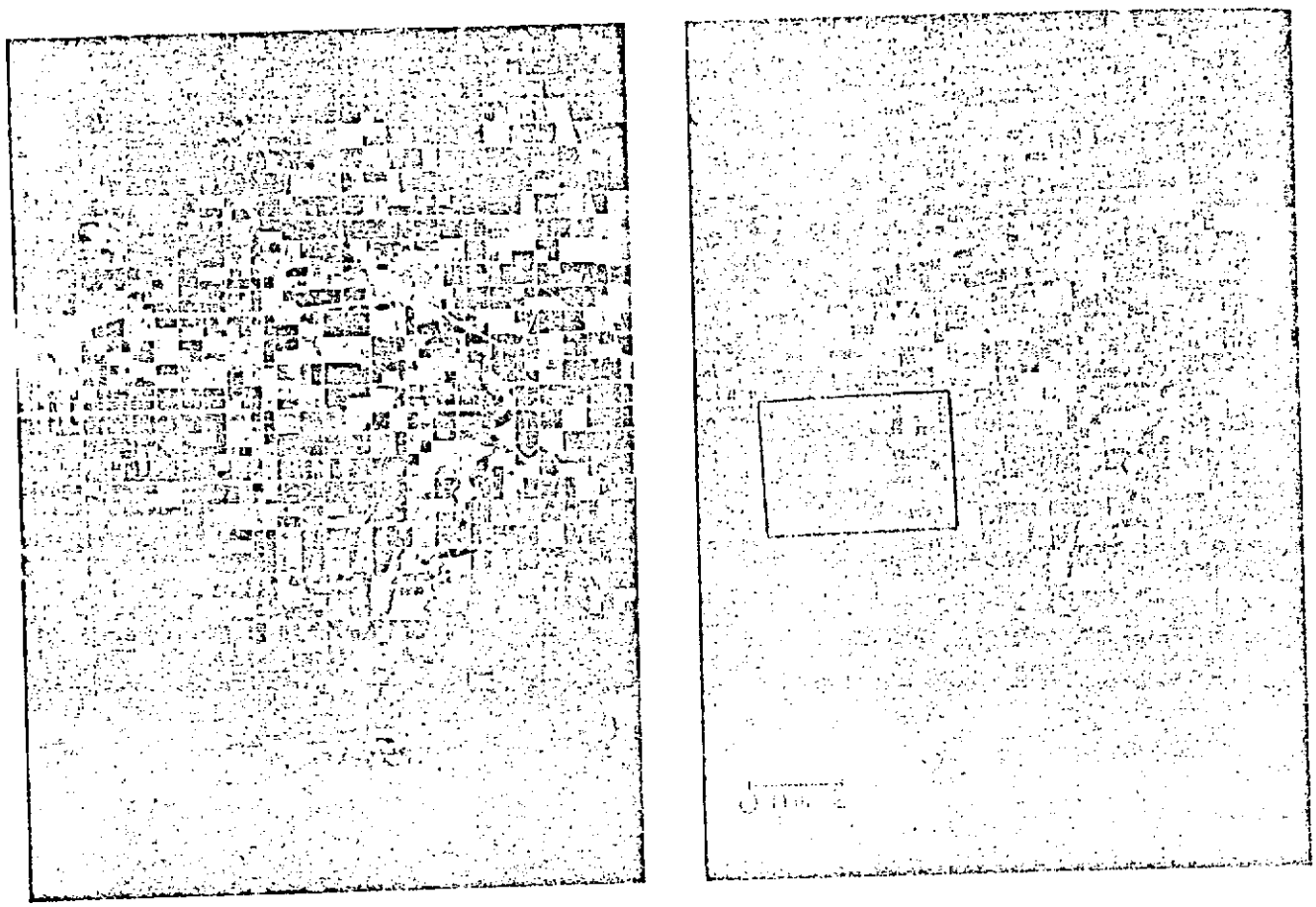

FIGURE 1. Representative examples of the high altitude multiband aerial photography of the Imperial Valley, California, used in this study. The above photographs are enlarged from 35 mm film format. Left is the Pan + 25A image; right is the IR + 89B image with the study area outlined. Not shown are the Pan + 58 and the Infrared Ektachrome images. Source: NASA.

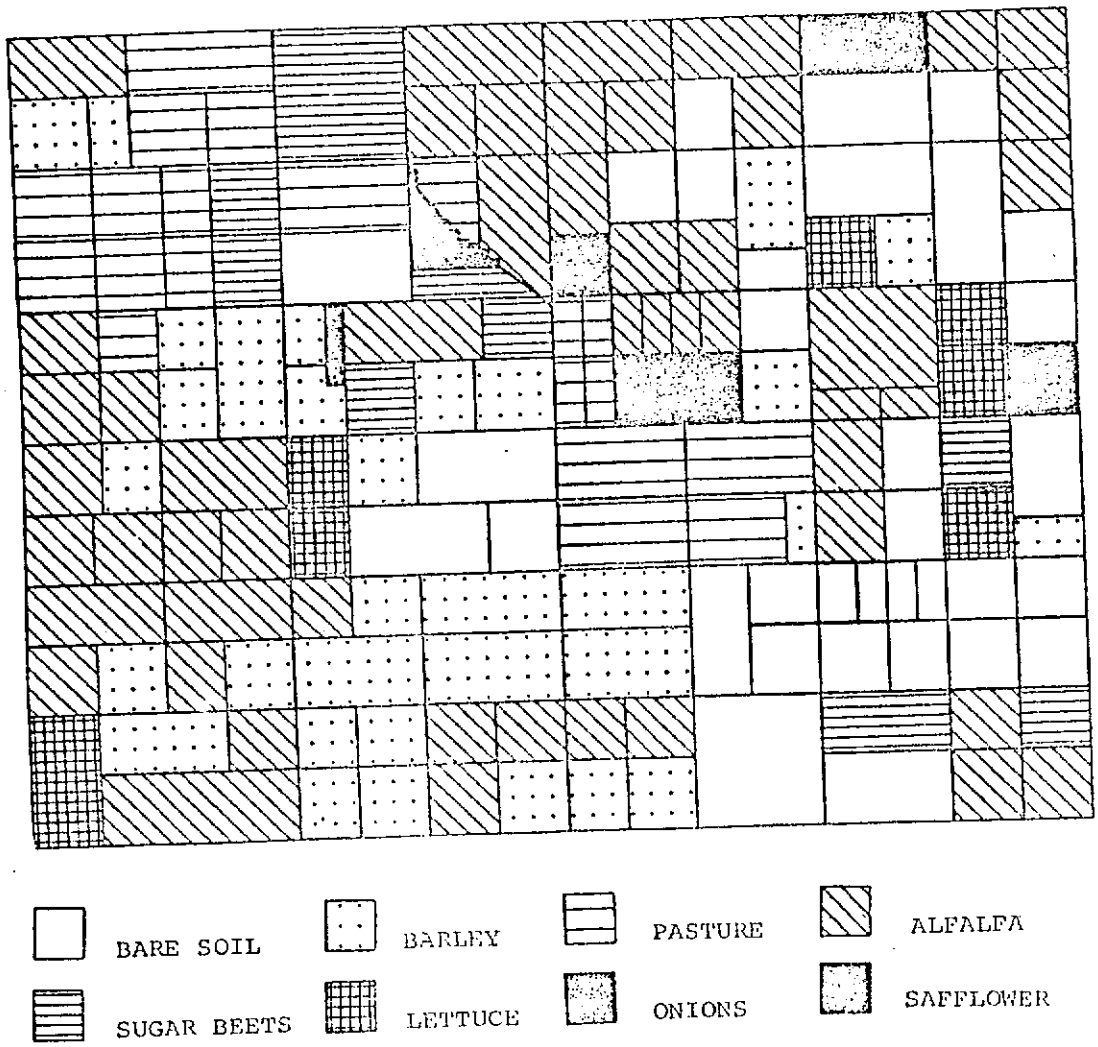

FIGURE 2. Land-use of the 160 fields in the twelve square mile study area in the Imperial Valley, California, as recorded by ground survey, March 8, 1969. (Note: On this map, Pasture and Rye have been combined. In the analysis Rye was combined with Alfalfa (Forage) as discussed in the text.)

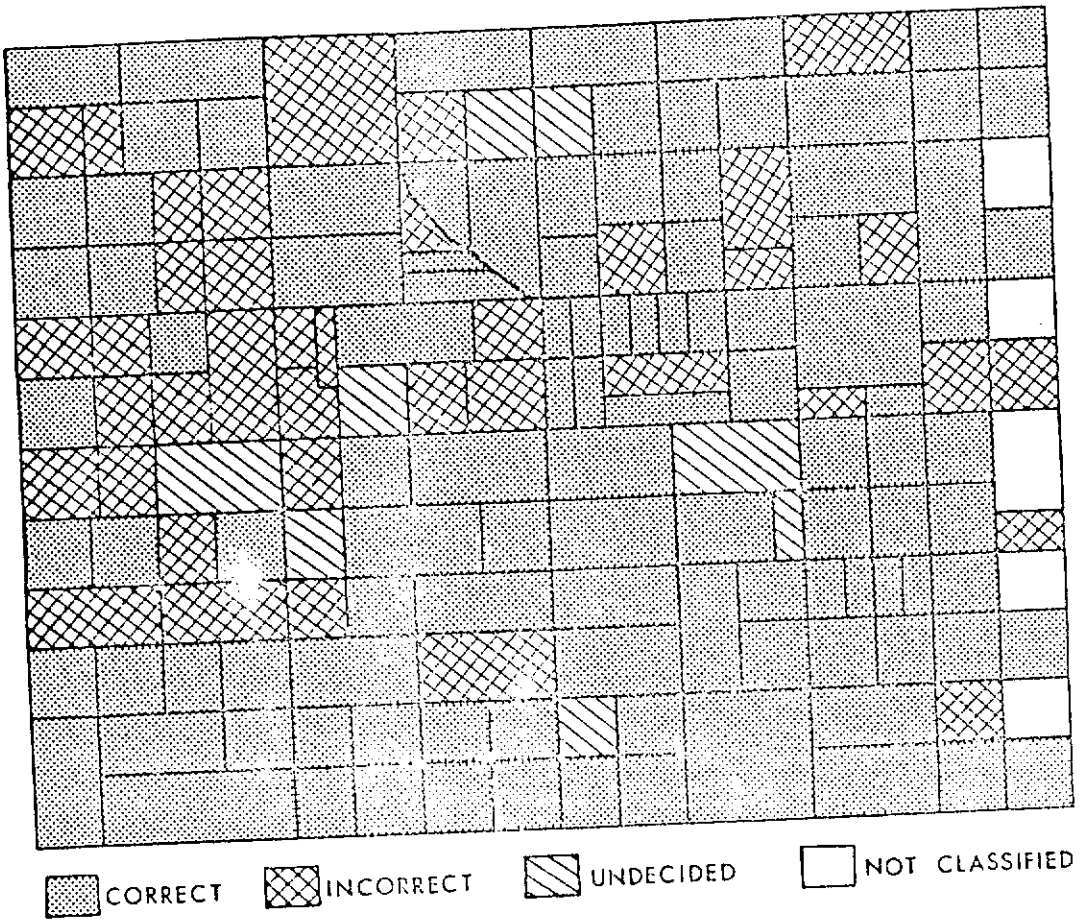

FIGURE 3. Location accuracy of the classification of the Infrared Ektachrome raw spot densitometric data, equal space quantized (prediction set). Of the 160 fields, 108 were correctly identified yielding a location accuracy of 68 percent.

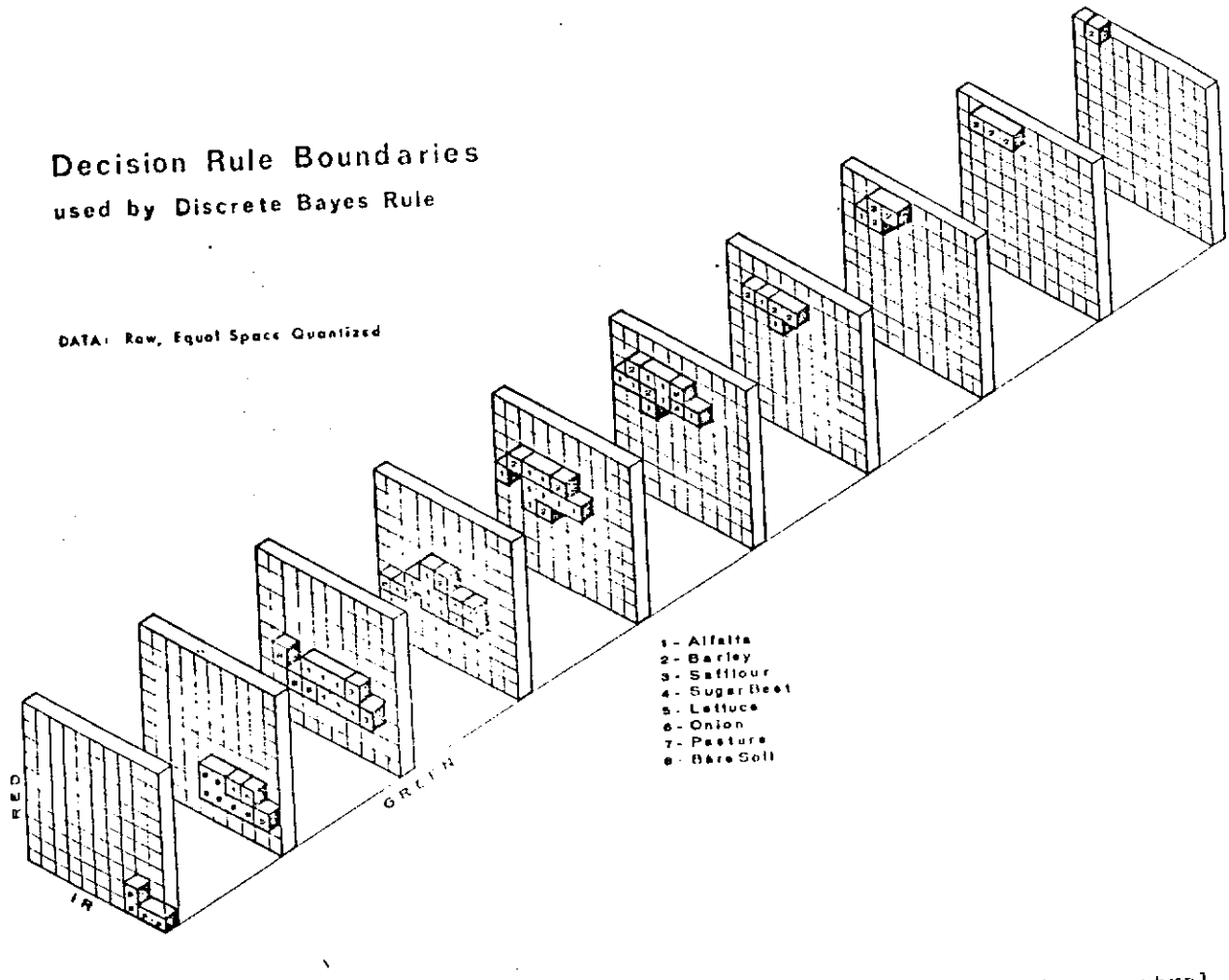

FIGURE 4. Viewed as an expanded cube, each dimension representing the spectral region of the three multiband images whose density values have been quantized to ten equally spaced levels, this sketch depicts the decision rule boundaries for each land-use category used by the discrete Bayes rule.